Nonlinear dynamics of heart rate variability during experimental hemorrhage in ketamine-anesthetized rats.

J E Skinner

Brian A. Nester DO, MBA
Lehigh Valley Health Network, Brian.Nester@lvhn.org

W C Dalsey

Published In/Presented At

Nonlinear dynamics of heart rate variability during experimental hemorrhage in ketamine-anesthetized rats

JAMES E. SKINNER,[1] BRIAN A. NESTER,[2] AND WILLIAM C. DALSEY[1]
[1]*Delaware Water Gap Science Institute, Bangor, 18013; and* [2]*Department of Emergency Medicine, Lehigh Valley Hospital, Allentown, Pennsylvania 18103*

Skinner, James E., Brian A. Nester, and William C. Dalsey. Nonlinear dynamics of heart rate variability during experimental hemorrhage in ketamine-anesthetized rats. *Am J Physiol Heart Circ Physiol* 279: H1669–H1678, 2000.—Indexes of heart rate variability (HRV) based on linear stochastic models are independent risk factors for arrhythmic death (AD). An index based on a nonlinear deterministic model, a reduction in the point correlation dimension (PD2i), has been shown in both animal and human studies to have a higher sensitivity and specificity for predicting AD. Dimensional reduction subsequent to transient ischemia was examined previously in a simple model system, the intrinsic nervous system of the isolated rabbit heart. The present study presents a new model system in which the higher cerebral centers are blocked chemically (ketamine inhibition of *N*-methyl-D-aspartate receptors) and the system is perturbed over a longer 15-min interval by continuous hemorrhage. The hypothesis tested was that dimensional reduction would again be evoked, but in association with a more complex relationship between the system variables. The hypothesis was supported, and we interpret the greater response complexity to result from the larger autonomic superstructure attached to the heart. The complexities observed in the nonlinear heartbeat dynamics constitute a new genre of autonomic response, one clearly distinct from a hardwired reflex or a cerebrally determined defensive reaction.

chaos theory; self-organization; surrogate controls

DESCENDING AUTONOMIC ACTIVITIES of higher cerebral origin are necessary and, in some cases, sufficient to evoke lethal cardiac arrhythmogenesis (3, 5, 9, 30, 33, 39, 46, 49) and myopathy (4, 8, 16, 18, 26). Indexes of heart rate variability (HRV) are currently thought to reflect this deleterious neural activity (42), and such indexes have shown promise as predictors of mortality in high-risk cohorts (17, 22, 25, 48). There is a problem, however, in trying to deal with the descending neural activities in a quantitative manner, because they are complexly regulated by the higher cerebral centers in parallel with the simpler homeostatic regulation by the brain stem. The higher neural centers, especially those involved in perception and defensive behaviors, can produce uncontrolled nonstationary effects in the heartbeat data.

The HRV indexes are based on stochastic models, each of which presumes that the variation of the heartbeats is randomly distributed around a mean (i.e., is noisy) and remains stationary throughout the interval of data collection. The potential for nonstationary neural regulation of the heartbeats plus the recent observations of their nonrandom variations suggest that the HRV measures based on the presumption of underlying stochastic dynamics may be inappropriate.

Nonlinear deterministic measures of the heartbeats have recently been shown to be more sensitive than the stochastic indexes in detecting the autonomic changes related to mortality (13, 19–21, 31, 33, 40, 41, 47). The primary explanation for the greater sensitivity is that the nonlinear measures are based on deterministic models, each of which presumes that the variation may be caused by a low-dimensional mechanism, not a high-dimensional stochastic process, and thus is a more appropriate measure (32, 38, 41, 47). Furthermore, some of the time-dependent nonlinear measures can treat the severe problem of data nonstationarity (32, 38, 41, 47).

What the time-dependent nonlinear algorithms show as indicators of cardiac vulnerability to lethal arrhythmias are transient nonstationary shifts of dimension of the heartbeat dynamics to a low value. This has been demonstrated in controlled data from conscious pigs undergoing experimental heart attack (32), in retrospective clinical data from patients with nonsustained ventricular tachycardia (NSVT) (38, 47), and in prospective clinical data from patients with chest pain and high-diagnostic risk (34). The significance of these low-dimensional excursions remains to be explained.

We previously studied dimensional reductions in a simple system model, the intrinsic cardiac nervous system of the isolated rabbit heart (40). We provided evidence that the system variables (inotropy and chronotropy) are measured by the subintervals of the electrocardiogram (ECG) (1/Q-T, 1/R-R–Q-T) and that they continue to undergo systematic nonlinear changes during stimulation by anoxia/ischemia. It was found that the system variables dissociate 2 min after the block of

---

Address for reprint requests and other correspondence: J. E. Skinner, Delaware Water Gap Science Institute, Bangor, PA 18013 (E-mail: sskinner@epix.net).

coronary flow but then reassociate, within 1 min, and manifest a new system attractor (an attractor is the geometric structure formed by the plot of the system variables).

We now report on a new model, one with a little more autonomic superstructure intact and one in which the perturbation of the cardiovascular system can be extended in time. Ketamine is known to block the N-methyl-D-aspartate (NMDA) receptors in the higher centers of the rat cerebrum (cortex, striatum, and hippocampus) (2), with only a small, stereospecific, cholinergic, inhibitory effect exerted directly on the heart (10). The rat is the animal of choice because of the large body of specific knowledge about its neurochemical centers and their stereotaxic accessibility. Specifically, we used this new model to test the hypothesis that the evoked nonlinear dynamics of the R-R intervals and of the Q-T and R-R–Q-T subintervals will be more complex in the ketamine-anesthetized rat than in the intrinsic cardiac nervous system.

METHODS

Data

Sixteen Sprague-Dawley rats (500 g males) were fed a standard laboratory diet and provided water ad libitum until the day of the experiments. The local Institutional Review Board approved our experimental protocol. The animals were treated humanely (Helsinki Animal Welfare Accords). Each rat was anesthetized intraperitoneally with ketamine (150 mg/kg) without respiratory assistance. Both femoral arteries were exposed and cannulated (polyethylene-50 tubing; Adams Intramedic). A heparin lock maintained cannula flow without systemic infusion. Arterial blood pressure was continuously monitored online, via the left femoral cannula, by using a calibrated strain gauge. The ECG was recorded continuously through needle electrodes inserted in the skin just above and below the heart [digitization 1,000 Hz/channel; bandpass 0.1 to 1,000 Hz; noise level 2-μV root mean square (RMS)].

Each rat was stabilized for 15 min after the surgery. After the recording of a 2.5-min control period, blood was then removed from the right femoral artery at a constant rate of 2 ml/min. The animals were bled to a mean arterial pressure between 30 and 35 mmHg for 15 min. The experiment was discontinued at 15 min, and the animal was euthanized by a barbiturate overdose (70 mg/kg).

Specific Analytic Algorithms

R-R interval determinations. The R-R intervals were determined algorithmically by a running 3-point convexity operator that has >95% correspondence to the nearest millisecond for visually determined intervals (29). The Q-T interval (Q peak to T end) used the maximum negative derivative in a forward-looking T window. T end was the first subsequent slope 40% greater than that of the maximum.

Correlation dimension. The three-dimensional algorithms all make similar correlation integrals (6, 35). They differ only in how the vector-difference lengths that form the integrals are added together [e.g., all of the vector differences, to increase signal-to-noise ratio, as in the classical correlation dimension (D2)] or in how the linear scaling region is determined [e.g., restricted in length, as in the point correlation dimension (PD2i)].

To make a correlation integral, the data are discretized (digitized) into a series of sequential data points (Pi), the total length (N) of which is, as a common rule, exponentially greater than the suspected dimension (e.g., $N > 10^{D2}$). R-R interval series are already discretized and thus do not require digitization. The next step is to determine the size of the embedding dimension (m), which is selected to be larger than the suspected dimension (e.g., $m > 2$ D2; for biological data this is usually $m = 2$–12). Multidimensional vectors must then be made from the data series and subtracted from one another to form the correlation integral. A small number of jumps over adjacent data points (jumps of size τ) are taken sequentially through the serial data to select data points, the values of which will then be used as coordinates to make the m-dimensional vectors ($\mathbf{V}_i$). Note that the values of i run throughout the data length, from $i = 1$ to N (almost N, minus the size of m). A second set of identical vectors are then made ($\mathbf{V}_j$), and, for a fixed value of i (e.g., $i = 1$, the first data point), all vector-difference lengths [$\mathbf{V}_j - $ fixed $\mathbf{V}(i = 1)$] are determined. Some of these differences will be large, but many (most) will be small. Then the next correlation integral ($\mathbf{V}_j -$ fixed $\mathbf{V}_i$, where $i = 2$) is made, and so on.

Each of the sequential correlation integrals, from $i = 1$ to $i = N - m$, is a function of time, because i is a function of time. To make the single D2 correlation integral, all possible vector difference lengths ($i = 1$ to $N - m$) are added together, so the D2 algorithm is not time dependent. For the pointwise correlation dimension (D2i), which is time dependent, only those vector-difference lengths for each fixed value of i are used to make the correlation integral.

The next step is to rank order the vector-difference lengths in each correlation integral. That is, the vector-difference lengths are ranked like small and tall soldiers on a marching field. Those who are the same size must stand behind the ones on the front row. Then the inspector general takes large even steps along the front row and counts how many soldiers are included within each step. He then plots the cumulative data (i.e., he adds new counts to the previous sum, C, for each new step size, R; the largest R includes all soldiers, the smallest only the shortest soldiers). Then he plots all C values versus R values on a log-log scale.

For nearly infinite data generated by a completely stationary system, a linear scaling region will be observed in the log-log plot, the slope of which will equal D2i, where i designates the point in time where the first point in the reference vector ($\mathbf{V}_i$) is located. If one combines all $\mathbf{V}_j - \mathbf{V}_i$ vector-difference lengths for all $\mathbf{V}_i$ sets of vector-difference lengths (i.e., from $i = 1$ to $i = N - m$), then the resulting log-log slope will equal D2. If one restricts the segment of the log-log slope of a single D2i to the smallest part of the scaling region that lies just above the unstable "floppy tail" (the latter is due to finite data length), then the slope will equal PD2i. The benefit of this latter restriction is that the slope is not contaminated by discretization noise in the smallest log-log region (floppy tail) and not contaminated by nonstationarities in the data that contribute to the larger log-log zone.

PD2i parameters. If one records from a sine-wave generator that is suddenly replaced by, e.g., a Lorenz chaotic generator, then a nonstationarity will occur in the data stream. Formally, the statistical properties of the data will be different the moment after the replacement. Our laboratory developed the PD2i algorithm to address data nonstationarity, because this problem invariably arises in long epochs of biological data when the system uncontrollably changes state (e.g., when shifting from sleeping to waking, or from quiescence to alerting). The first insight that led to our algorithm was that in nonstationary data, the vectors made from

"points" of data that are stationary with respect to the "point" the reference vector is in (a "point" is a small strip of data, $m \times \tau$ data points long) will contribute uncontaminated vector-difference lengths only to the small $\log - R$ part of the scaling region.

We found that this restricted segment could be defined by a linearity criterion (LC) and a plot length (PL) criterion. The LC enables the detection of the upper limit of the floppy tail and the PL sets the upper limit of the restriction (usually 15%, starting from the small $\log - R$ end). To prove that this insight about the restriction was valid, we tested the PD2i algorithm in obviously nonstationary data made from concatenated samples of sine, Lorenz, Henon, and random data. We found that the mean PD2i of each subepoch had an error that was < 4% of that made by D2 for the stationary variety of the data (35).

The parameters used in the current study were PL = 0.15, LC = 0.3, convergence criterion (m vs. slope) = 0.4, and T = 1 (time delay = 1 beat). These are the same PD2i settings used previously by our laboratory in both animal (32, 35, 37) and human (34, 38, 47) studies.

Surrogate controls. Any nonlinear algorithm suffers from its sensitivity to stochastic noise. R-R data contain discretization errors (0.2% for 1,000 Hz digitization of the ECG) and amplifier noise (~2 mV, RMS). Each R-R interval was therefore expressed as 0.5 integer/ms, because this enables a small amount of noise in the R-R data to be tolerated by the PD2i algorithm (35).

To estimate the contribution of noise, the method of surrogates (44, 45) was used. Algorithms were run on each R-R file and on a phase-randomized surrogate made from the same file. The surrogate enables the test of the null hypothesis that a linear stochastic process can explain the data, that is, if the data can be presumed to be noise free.

Statistics

Paired t-tests were used to assess the within-subjects shift in PD2i dimensions evoked by the hemorrhage. We could not adequately justify the presumption that changes between subjects would occur uniformly across all subjects, because we do not know what PD2i measures and what effects small differences in initial conditions might have. Therefore, analysis of variance (i.e., within and between subjects) was not used. Alternatively, the nonparametric binomial probability statistic was used to assess significant time-dependent changes for the study group (α, $P < 0.01$). Parametric t-tests were used to compare R-R data with their surrogates because these had >1,000 data points each and normal distributions. One-tailed α-levels were used for the surrogate tests, because the null hypothesis is directional. Correlations between the PD2i measure of HRV and those measures based on a stochastic model were assessed within subjects by the Pearson product-moment coefficient. After α-testing, the β-power was examined (β, $P > 0.90$) using the proportions method of Fleiss (7).

RESULTS

Each rat was bled to a final mean arterial pressure between 30 and 35 mmHg, accomplished within a period of 15 min. The blood pressure drop during the first few minutes was not as great as that during the last few minutes (i.e., it was nonlinear). Although all animals remained in the anesthetized state, it was noticed that some were more reactive to a tail pinch than others, but this was not studied systematically. None of
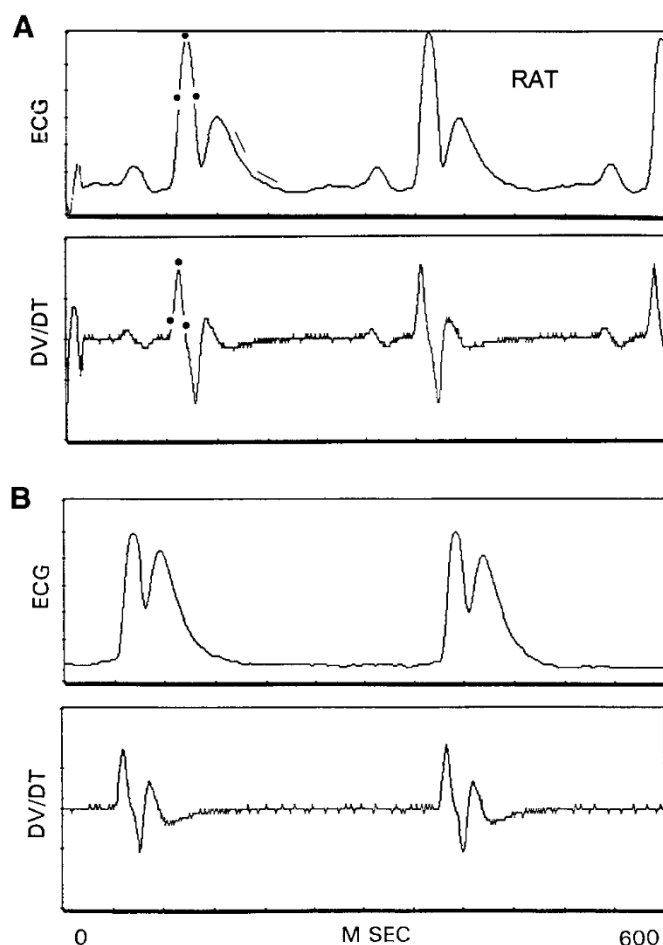

Fig. 1. Electrocardiogram (ECG) recorded from the ketamine-anesthetized rat before (A) and after (B) 5 min of blood loss at 2 ml/min in a 500-g rat. The first derivative (DV/DT) is also shown below each ECG. ●, Position of the 3-point convexity operator at its maximum output; slope lines indicate maximum negative DV/DT in T window and its subsequent increase by 40% (T end).

the rats appeared to suffer labored breathing or respiratory distress during this 15-min period.

Figure 1 shows the effects on the rat ECG of 5 min of blood loss (2 ml/min, 500 g). Note that although the experimental shock results in a reduction of the R wave and an increase in the T wave, there is still ample amplitude for discrimination of the two peaks.

Figure 2, *top*, shows the effects of slow, continuous hemorrhage (downward arrow, 2 ml/min blood loss) on the R-R, Q-T, and R-R–QT intervals in the ketamine-anesthetized rat. The infrequent abnormal beats on the Q-T trace are due to small movement artifacts. Such inaccuracies always lead to rejection of the PD2i at these locations in the data stream. The rejection occurs because the presence of the artifact as a coordinate in the reference vector leads to failure of one or more of the scaling criteria.

The PD2i of the R-R intervals is shown in Fig. 2 immediately below the R-R and subinterval traces (*middle*). The mean value for the light-anesthesia control period (A) is ~3.1 dimensions (i.e., degrees of freedom). During the 2.0-min period after the hemor-
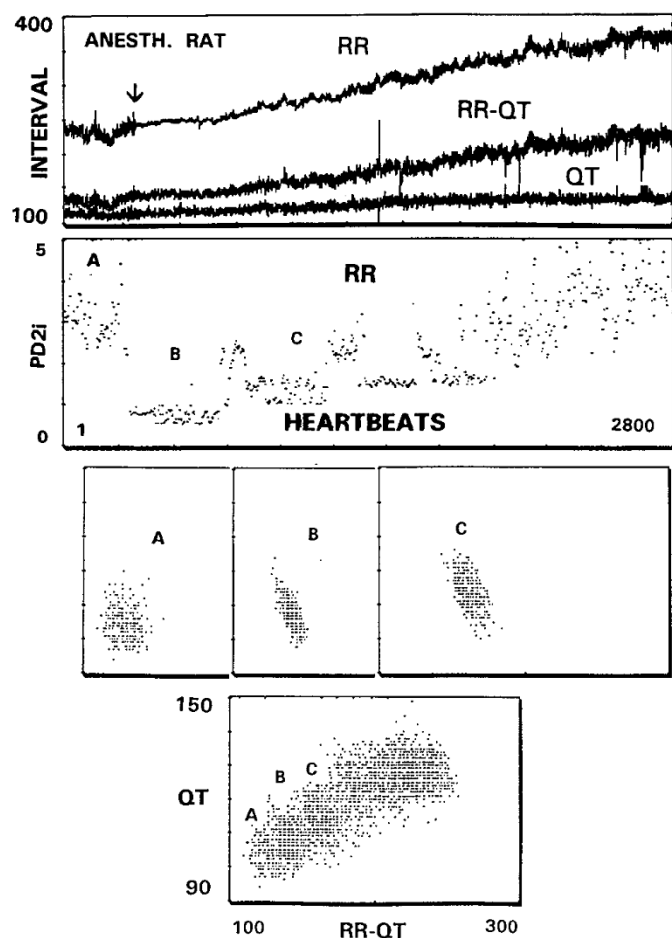
Fig. 2. Interval series (INTERVAL, in ms), time-dependent dimensions (point correlation dimensions; PD2i), and attractors (QT vs. RR-QT, in ms) in the ketamine-anesthetized rat during experimental hemorrhagic shock (arrow, 2-ml/min blood loss). Subepochs indicated in the PD2i trace are shown for attractors A, B, and C separately (*third row*) and all of them together, sequentially (*fourth row*). Heartbeats shown (2,800) consumed 14.0 min of time. See RESULTS for more information.

rhage was initiated (B), there was an immediate and relatively stable reduction in the dimension of the R-R interval series to a mean of 0.8 (1.01 grand mean for all rats, $P < 0.01$, binomial probability, paired t-test). This subepoch was also associated with a marked reduction in the standard deviation of the R-R intervals, as can be seen graphically in Fig. 2, *top*, just after the downward arrow. At 2.2 min after the hemorrhage was initiated, there was an abrupt rise in dimension followed by what appeared to be a series of "dimensional oscillations" for the next 2.3 min (C). These fluctuations, 4.5 min after the initiation of hemorrhage, abruptly rose in dimension for a prolonged period and then decreased to a rather steady level of 1.6 dimensions for a while. At 8.5 min there began a rather wild series of dimensional fluctuations that slowly rose to a mean of 4.0 by 15 min (3.22 grand mean for all rats, $P < 0.01$, paired t-test).

Figure 2, *bottom*, shows the joint plot of the Q-T versus R-R–Q-T subintervals for each heartbeat dur-

ing the whole experiment. The *points A, B,* and *C* are shown in the three smaller panels above it. Because Q-T versus R-R–Q-T is a plot of the 1/inotropy versus 1/chronotropy variables that regulate the heart, it is a way to show the system attractor (an attractor is a multidimensional plot of the system variables that specifies its dynamics over all time). During the control period (*subepoch A*), when the PD2i is around 3, the Q-T versus R-R–Q-T points fluctuate around the center of mass and form a "fuzzy ball" (i.e., the dots are space filling in 3 dimensions). During the *subepoch B* period, when the dimension is around 1, the points move up and down negative-sloped lines, each of which has similar slopes (see Fig. 3). During the *subepoch C* interval, when the oscillations between 1 and 2 dimensions began, there is a change in the negative sloped lines (1-dimensional) to those of a "zigzag" pattern (i.e., space filling in 2 dimensions).

This zigzag pattern is seen in more detail on the expanded time base of Fig. 3. The same R-R and PD2i series are shown for the *subepoch C* as in Fig. 2, but now the "dimensional oscillations" are more easily seen as systematic changes from higher to lower values. Four parts of the first two cycles are indicated (A–D). The Q-T versus R-R–Q-T plots (attractors) are shown in Fig. 3, *bottom*, for each of the A–D periods. During the first half cycle, when the dimension is around 1 (A), the plot of Q-T versus R-R–Q-T is a thin negative-sloped line. During the second half cycle (B), when the dimension is closer to 2, the plot becomes space filling in two orthogonal directions. That is, a zigzag pattern

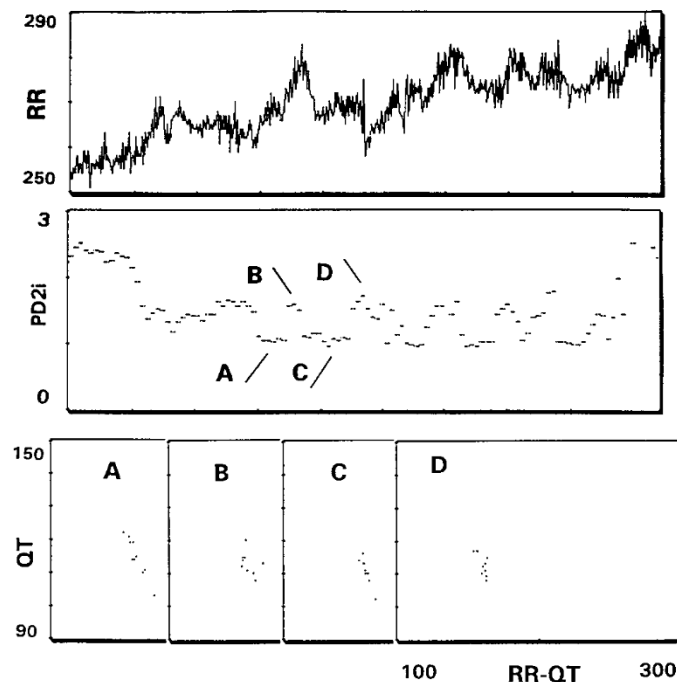Fig. 3. Expanded time base for R-R intervals and corresponding PD2i values of the *subepoch C* shown in Fig. 1. In the PD2i trace, A–D indicate four halves of the first two cycles of the "dimensional oscillations." The attractors (Q-T vs. R-R–Q-T) for each half cycle are shown in the *bottom row*. R-R values are in milliseconds, and PD2i values are in dimension. See RESULTS for more information.
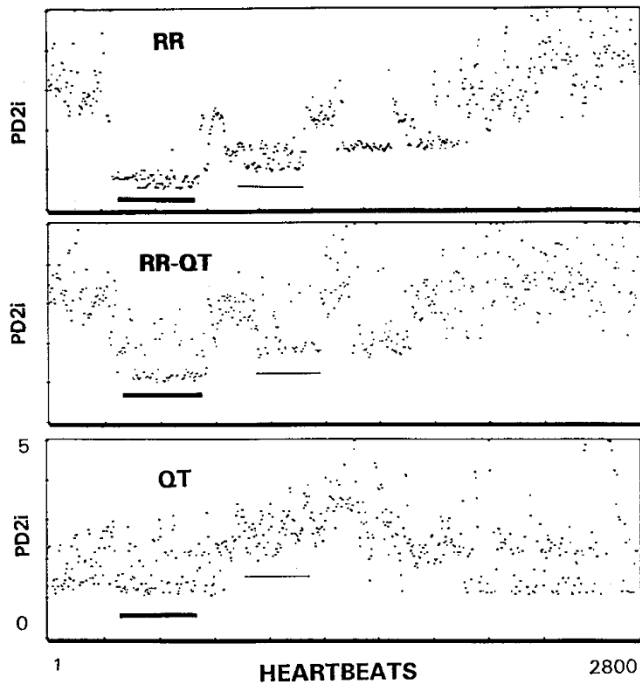
Fig. 4. Time-dependent dimensions (PD2*i* values) for the R-R intervals and their corresponding Q-T and R-R–Q-T subintervals during blood loss. Ordinates are 0 to 5 dimensions. Dark line is *subepoch B*, and thin line is *subepoch C* (see RESULTS).

is observed when the dots are interconnected, as in the letter Z. This same pattern is observed during the next cycle (*C, D*), and so on.

Figure 4 shows the PD2*i* of the R-R data series (*top*) and each of the concomitant subinterval series, Q-T (*bottom*) and R-R–Q-T (*middle*). During the *subepoch B* (dark underline), all three series have approximately the same lower dimension, around 1. During *subepoch C*, especially during the dimensional oscillations seen in the R-R series (thin underline), there is a dissociation of the mean PD2*i* values. The mean for the Q-T series is considerably higher (most PD2*i* values > 2.0) than that for the R-R–Q-T series (most PD2*i* values < 2.0).

Table 1 shows the composite results for the 16 rats during hemorrhagic shock. Three of the rats (indicated by *rats 6, 9,* and *10*) did not show any dimensional variation during the bleeding; one of these (*rat 6*) showed relatively high ventricular ectopy during the control condition. We have no explanation for the lack of variation. Of the remaining 13 rats, none showed any ectopy, but some did show twitch movement artifacts. In these 13 rats, each manifested a lower dimension during the first few minutes after the start of the bleeding than it did during the previous control period observed during light anesthesia ($P < 0.01$, binomial probability test, paired *t*-test). Many of these rats, however, did not manifest the normal unanesthetized PD2*i* level of ~3.0 during the control period, but rather showed reduced dimensional levels.

The dimensional reduction within 2 min after the start of bleeding was to a level of ~1.0 (grand mean

equals 1.0). As seen in both Table 1 and Fig. 5, as the hemorrhage progressed, there is a systematic rise in dimension to larger values by the end of the 15-min experiment (grand mean equals 3.4, $P < 0.01$). Most animals showed at least one "dimensional oscillation" during the interval between 2.0 and 4.5 min after the start of the bleeding (designated by Y). In some, however, the PD2*i* values during this interval either linearly elevated (e.g., Fig. 5, *rat 5*) or stayed constant, without any characteristic cycling or wandering behavior. Of those that did show the cycling, there often occurred a large initial dimensional increase, as seen in Fig. 2 (*middle panel*, between the *subepochs B* and *C*) and in Fig. 5 (after the *B* interval, *rat 7*). This large cycle was then followed by one or more smaller-amplitude dimensional oscillations.

Figure 5 shows the R-R values and associated PD2*i* values for six rats that had very few cardiac arrhythmias and movement artifacts. These were selected because the application of stochastic HRV measures requires absolute data stationarity. To make comparisons between PD2*i* and other HRV measures, three

Table 1. *Composite data from the 16 rats recorded before and after continuous hemorrhagic bleeding at 2 ml/min*

Rat No.	Mean PD2*i*			Oscillation in PD2*i* C
	A	B	D	
1	3.1 ± 0.7	0.8 ± 0.3*	3.6 ± 0.9‡	Y
2	2.1 ± 0.7	1.1 ± 0.6*	2.0 ± 0.5‡	Y
3	1.7 ± 0.6	1.4 ± 0.6	2.8 ± 0.5‡	Y
4	2.5 ± 1.4	1.1 ± 0.5*	3.8 ± 0.6‡	Y
5	0.6 ± 0.1	0.6 ± 0.7	3.9 ± 0.8‡	N
6†	4.2 ± 0.4	3.8 ± 1.4	4.4 ± 0.7	N
7	2.7 ± 1.0	0.97 ± 0.1	1.9 ± 1.5	Y
8	4.9 ± 0.2	0.7 ± 0.2*	2.7 ± 0.3	Y
9†	3.2 ± 0.9	4.3 ± 0.3	3.9 ± 0.6	N
10†	1.4 ± 0.4	1.0 ± 0.2	1.3 ± 0.5	N
11	0.7 ± 0.1	0.7 ± 0.1	3.4 ± 0.5‡	Y
12	0.9 ± 0.8	0.9 ± 0.7	3.7 ± 0.9‡	Y
13	0.9 ± 0.3	0.8 ± 0.3	4.6 ± 0.9‡	Y
14	0.9 ± 0.6	0.7 ± 0.1	2.4 ± 1.7‡	Y
15	1.0 ± 1.6	0.8 ± 0.1	4.7 ± 1.3‡	Y
16	0.9 ± 0.4	1.1 ± 0.9	4.6 ± 0.6‡	Y

Values are means $\pm$ SD. Each column entry shows the mean dimensional values and their standard deviations during each of the following subepochs: *A,* previous control, 2.5 min; *B,* 0–2.5 min after start of bleeding; *D,* 12.5–15 min after start of bleeding. The presence of one or more cycles of oscillation in *subepoch C* (2.5–5.0 min after start of bleeding) is indicated (Y = yes, N = no). All point correlation dimension (PD2*i*) means in *subepoch B* are statistically significantly different from their randomized-phase surrogates. The surrogates all had large means, in the range of 6–7 dimensions, with standard deviations being approximately the same. Both the natural and surrogate distributions appeared to be Gaussian. *$P < 0.01$ (paired *t*-test, $\alpha < 0.01$, $\beta > 0.90$), *subepoch B* entries compared with corresponding values in *subepoch A;* also, *subepoch B* is significantly different from *subepoch A* by the binomial probability test (only 2 of 16 increases implies $P < 0.01$). †No significant changes of *subepoch A* compared with *subepoch B* or *subepoch D; rat 6* had numerous ventricular ectopic beats in the control condition. Lack of variation in others is unexplained. ‡$P < 0.01$ (paired *t*-test, $\alpha < 0.01$, $\beta > 0.90$), *subepoch D* entries compared with corresponding values in *subepoch B;* also, *subepoch D* is significantly different from *subepoch B* by the binomial probability test (only 1 of 16 decreases implies $P < 0.001$).

Fig. 5. R-R intervals and corresponding PD2i values for 6 rats without cardiac arrhythmias or movement artifacts during hemorrhage. Each trace shows 2,800 R-R intervals. The total time intervals for traces are the following: *rat 1* = 14.0 min, *rat 7* = 11.3 min, *rat 5* = 18.7 min, *rat 8* = 9.8 min, *rat 12* = 10.8 min, and *rat 13* = 10.2 min. All calibrations are the same as indicated at *top left* (R-R in ms; PD2i in dimensions), except for *rat 5*, in which R-R is 200–500 ms. The horizontal lines indicate the selected stable PD2i subepochs selected for stochastic-measure analyses (see Table 2).
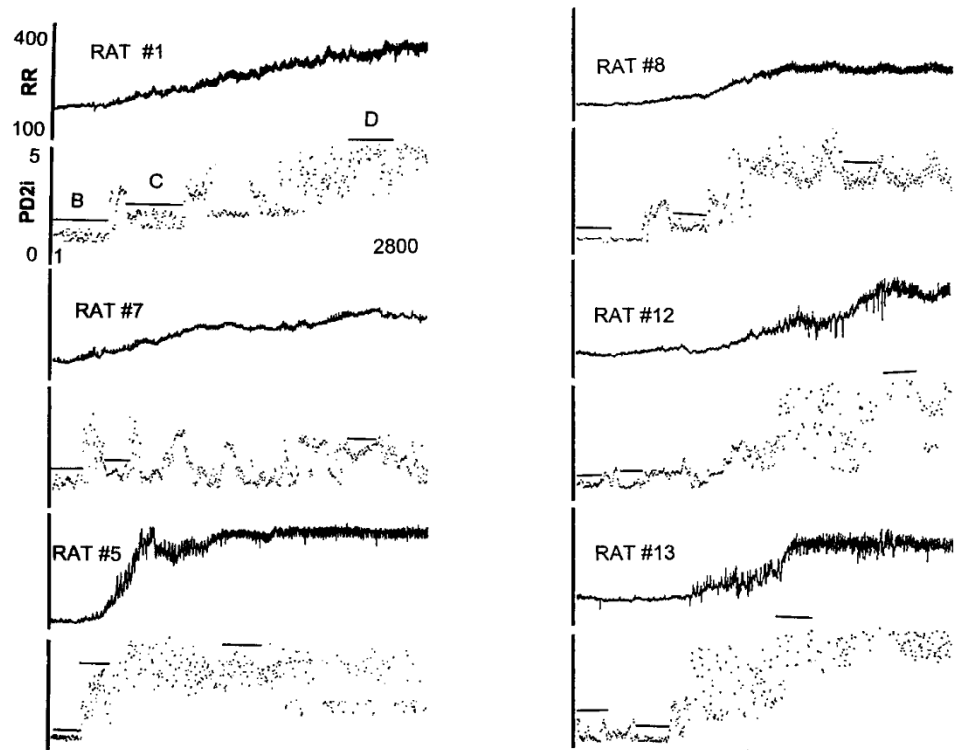
intervals were selected for each animal during relatively stable (stationary) periods of their respective PD2i values (Fig. 5, *B–D*). The correlation coefficients between the PD2i and each of the other standard measures of HRV are shown in Table 2.

DISCUSSION

Significance of a Low-Dimensional Excursion

What we want to understand is the significance of the "low-dimensional excursion" observed in the heartbeat dynamics of the patient with NSVT (38) or the pig with left anterior descending coronary artery occlusion (32). This single physiological event is the harbinger of the onset of ventricular fibrillation. What causes it and what does it mean mechanistically?

Our previous study (40) discovered that in the isolated heart, a simple way to examine the system variables (i.e., inotropy and chronotropy) was through the heartbeat subintervals. We first noted that the Q-T subinterval is shortened by stimulating single sympathetic nerve fibers projecting to the ventricles (15) and is inversely related to inotropy as measured by intramural pressure. The R-R interval (chronotropy) appears to be regulated independently by nerve fibers projecting to the atria (14). Because the R-R variation also contains that of the Q-T variation, we proposed that the R-R–Q-T subinterval (i.e., the diastolic interval) would best serve as the independent measure for chronotropy and thus be the variable necessary for exhibiting the system attractor.

We found in the intrinsic cardiac nervous system that a dimensional decrease in the heartbeat dynamics

occurred when the afferent-efferent neural loops began to change such that the relationship of the system variables exhibited a new system attractor (40). The changed shape of the system attractor indicated a new physiological function, for example, a shift from cardiac output preservation to cardiac energy preservation (40). Each change in the attractor was announced by a transient dimensional increase-decrease (i.e., a single cycle), and it occurred about once every 2 min.

In this study we found evidence of more rapid cycles (i.e., dimensional oscillations) that can occur on the order of tens of seconds (40–50 heartbeats). The system attractors exhibited in the subinterval plots (Figs. 2 and 3) show a change back and forth from a function that preserves cardiac output (1-dimensional, negative-sloped line attractor) to one that both preserves cardiac output and preserves cardiac energy (2-dimensional, zigzag attractor). As seen in Fig. 5, there is a wide variation in both the number and magnitude of these dimensional cycles.

The wide variety of individual patterns of dimensional change observed among the ketamine-anesthetized rats was not observed among the isolated rabbit hearts. The latter more or less showed similar attractor changes over time (40). The rich pattern of individualized variation seen in the present study with the brain stem intact could explain why the PD2i of the heartbeats is not correlated with any stochastic measures in other studies (32, 34, 38). If, in the present study, we had not selected the stable PD2i intervals, then the correlations with the stochastic measures would not have been high. That is, the mean PD2i

Table 2. *Correlation coefficient of mean PD2i of R-R intervals with SD PD2i, mean NN, SD NN, peak LF, or peak HF during hemorrhage shock in the ketamine-anesthetized rat*

| Subepoch | PD2i | | NN | | | |
	Mean, dimensions	SD, dimensions	Mean, ms	SD, ms	*Peak LF, ms²/Hz	*Peak HF, ms²/Hz
Rat 1						
B	0.82	0.31	252	2.9	4,000	4,000
C	1.30	0.38	273	3.6	4,500	2,000
D	3.61	0.90	361	6.6	9,000	6,500
Rat 7						
B	0.92	0.14	154	2.5	5,000	4,000
C	1.31	0.19	182	3.7	5,000	4,800
D	1.94	0.15	294	4.4	3,200	2,800
Rat 5						
B	0.63	0.70	208	1.8	3,400	2,900
C	1.99	0.68	217	5.7	24,000	19,000
D	3.90	0.76	452	7.0	10,000	7,000
Rat 8						
B	0.67	0.23	150	1.3	1,500	500
C	1.09	0.14	171	3.1	2,500	1,400
D	2.72	0.26	245	6.1	9,000	6,000
Rat 12						
B	0.89	0.66	164	2.9	3,000	1,000
C	0.90	0.24	168	3.9	5,000	2,400
D	3.74	0.91	251	11.9	20,000	16,000
Rat 13						
B	0.77	0.28	161	2.7	900	900
C	0.54	0.06	158	1.9	4,600	1,000
D	4.63	0.89	316	10.9	3,800	4,000
Correlation with PD2i						
R^2		0.51	0.63	0.86	0.22	0.25
$P <$		0.009	0.001	0.001	0.047	0.033

Ketamine-anesthetized rats (500 g) had blood removed at a rate of 2 ml/min. The 6 rats were selected from among the 16 because each had very few cardiac arrhythmias and/or movement artifacts (i.e., the R-R intervals were stationary over sampled heartbeats). Stable PD2i subepochs were then selected from each R-R series after the onset of blood loss. The specific subepochs are indicated in Fig. 5 (*B, C, D*), where *B* is within 0–2 min, *C* is within 2–4 min, and *D* is after stabilization of the final R-R level. R^2, correlation coefficient; NN, normal-to-normal beats. *When multiple peaks were in the low-frequency (LF) (0.04–0.15 Hz) and high-frequency (HF) (0.15–0.40 Hz) bands, the one with the largest amplitude was selected.

values could have been quite different, larger or smaller, because of the nonstationarities within them. The poorer correlations between PD2i and the power spectra were because of the brevity of the stationary data lengths (i.e., there were not enough samples to adequately resolve the lower frequency spectra).

The intrinsic cardiac neurons, many located in the "fat pads," provide afferent-efferent regulations similar to those observed with the neural superstructure intact (1, 14, 15, 27, 28), but certainly the brain stem autonomic centers are there for some evolutionary reason. Ketamine is thought to be an anesthetic that targets the NMDA receptors that are mainly located in the higher central nervous system (cortex, striatum, and hippocampus) (2), thus leaving the cardioregulatory centers in the brain stem relatively intact. This is not to say that ketamine has no other effects, for it does produce a small amount of stereospecific inhibition of cholinergic re-uptake in the isolated heart (10). But certainly, it would seem reasonable to say that the ketamine-anesthetized rodent has a larger autonomic structure attached to its heart compared with the intrinsic cardiac nervous system that remains when the heart is surgically isolated.

It is not surprising that the more complex neural superstructure is related to a more complex dimensional response, but it is surprising that it is associated with rapid oscillations of multiple cycles. It is also surprising that brain stem autonomic complexity underlies such a rich variety of individualized nonlinear response patterns (Fig. 5).

The PD2i Algorithm and Data Nonstationarity

Mathematically, the dimension of the attractor reconstructed from a multidimensional plot of the data stream (the reconstructed attractor) and that observed after plotting the independent variables (the system attractor) become equal in the limit (43). The proof of this convergence is the basis for the algorithm of the correlation dimension (D2) (11). When applied to biological data, however, a problem with D2 arises. The algorithm requires data stationarity (impossible to achieve) and long data length (even more impossible to achieve without nonstationarities). The point correlation dimension (PD2i) is an algorithm similar to D2 and D2i that we developed to treat the problem of data nonstationarity (37).

The unique feature of the PD2i is the restriction of the scaling region to a small log − R part of the correlation integral (see METHODS). It has been demonstrated in nonstationary concatenated data that PD2i

has only a 4% error compared with D2 values made with corresponding samples of stationary data of long length (37). It is this treatment of the problem of nonstationarity that, in part, may explain why the PD2i algorithm is so much more sensitive in predicting mortality among high-risk patients than other linear and nonlinear algorithms (37, 38, 41).

What is Significant About Low-Dimensional Excursions Below 1.2?

In conscious pigs undergoing experimental heart attack, it was shown that the PD2i of the R-R intervals dropped below 1.2 dimensions within the first minute of occlusion, but only in the pigs that later manifested ventricular fibrillation (VF) (i.e., at around 16 min) (32). In the pigs with 50–90% occlusions of the left anterior descending coronary artery, which did not manifest VF within 24 h, the PD2i remained above 1.2 at all times. What the significance is of this particular 1.2 level is not yet known.

This result, however, was later confirmed in retrospective data from patients with NSVT who either died of VF on the day of their recording or did not die within at least 3 years. In 100% of the VF subjects there was found to be a low-dimensional excursion to or below 1.2 at least once every 15 min throughout the period of their Holter recording (38, 47). In the NSVT subjects who did not die, none showed any low-dimensional excursions below 1.2.

Our studies of R-R interval dynamics in the human transplanted heart (23, 24) show that cardiac denervation leads to a heartbeat dynamic of almost precisely 1.0 dimension. That is, a single variable appears to regulate changes in heart rate. This dimensional level is to be distinguished from those fractional dimensional ones, observed in the present and other studies, which are associated with cardiovascular risk (e.g., myocardial ischemia, hemorrhagic shock). The transplant studies, however, do show that the higher dimensions require descending neural projections to the heart.

The low-dimensional excursions observed in our previous studies in pigs (32) and humans (34, 38, 47) are on the same order of magnitude as those seen in Figs. 2–5. These excursions often resemble the dimensional oscillations (seen in the present study). In all of these cases the dimensional response is rapid, occurring within seconds after the onset of the cardiovascular event. The effects of psychosocial stressors and other higher central perturbations (e.g., pathway blockade) are known to be quite rapid in reducing R-R interval dimension (3, 32–34), and thus descending projections from higher neural systems could be an explanation for the early and rapid low-dimensional responses.

We do not yet know what the mechanism is for the fractional low-dimensional excursions. Furthermore, we cannot yet interpret what the significance is of any dimensional level. Other physiological systems, however, may relate to these rapid fractional shifts observed in the heartbeats.

Response Cooperativity

Recent studies of event-related potentials in the brain suggest that low-dimensional excursions occur after a period of learning (35, 36). Furthermore, at least for some types of rhythmic extracellular activities, the low dimension is temporally associated with a spatially distributed "response synchrony" in which the neurons in the local ensembles become momentarily brought into a global phase alignment (36). This engendered relationship among the neurons is similar to the "cooperativity" of musicians playing in a small ensemble. A simpler metaphor is that of multiple crank turners of an old-fashioned sine-wave generator.

If three independent persons are turning the crank together, a rather jittery sinusoid will result having three degrees of freedom (PD2i = 3), but if the crankers follow a leader (internal or external), then the output will systematically return to a smooth sinusoid having a dimension of 1. The dimension (degree of jitter in the data stream) is therefore related to the cooperativity that exists among the components of the generator mechanism (24, 35).

In the control of the heartbeats, the representation of the crank turners would seem to be the large number of afferent-efferent loops contained within the autonomic nervous system. The following representations show examples of such loops: *1)* those intrinsic to the small neuropil located in the heart; *2)* those that loop from the peripheral receptors through the brain stem and back to the periphery; and *3)* those that loop through the frontal granular cortex and amygdala and are known to control myocardial vulnerability to lethal arrhythmias in conscious pigs. By analogy with the cerebral control of cooperativity, some self-organized mechanism for the global control of phase among these afferent-efferent loops of the autonomic nervous system could be the basis for the rapid low-dimensional phenomena exhibited in this and other studies.

What is important to realize about all of these new data is that a new genre of response is exhibited in the nonlinear activities. The response is neither an autonomic reflex (i.e., homeostasis) nor an autonomic reaction to support survival behavior (i.e., cerebral defense). What is evoked is a complex autonomic adaptation to a strong stimulus event that may involve the self orchestration of large numbers of afferent-efferent loops in the continuous systematic control of nonlinear behavior.

We call the response an adaptation because it requires, like a Darwinian system, experience with its environment. The adaptive mechanism for hemorrhagic shock may result from some learning-dependent mechanism similar to that involved in "cardiac preconditioning." In this latter example, recent experience with anoxia/ischemia results in a smaller sized infarction (i.e., when a coronary artery is tied off), because of inhibitory *g* protein-dependent downregulation of the adenosine receptor (12). Such self-adaptive changes in the underlying neurocardiac mechanism may explain

the rich variety of nonlinear responses (Fig. 5) observed in the R-R intervals during hemorrhage.

In conclusion, we now believe that the low-dimensional excursions occur when the nonlinear dynamics within the autonomic nervous system self-organize to change a physiological function that will lead to survival. This adjustment is like a Darwinian adaptation, but on a small time scale. All subdivisions of the autonomic nervous system appear to be capable of undergoing this self-organization (e.g., those neurons intrinsic to the heart, as well as those that loop through the brain stem). The present study shows that the larger the neural superstructure attached to the heart, the more rapid and complex the adaptation. The complex nonlinear regulation constitutes a new genre of autonomic response, one clearly distinct from a hard-wired reflex or a cerebrally programmed defensive reaction.

REFERENCES

1. **Armour JA.** Peripheral autonomic neuronal interactions in cardiac regulation. In: *Neurocardiology,* edited by Armour JA and Ardell JL. New York: Oxford University Press, 1994, p. 219–244.

2. **Bresink I, Danysz W, Parsons CG, and Mutschler E.** Different binding affinities of NMDA receptor channel blockers in various brain regions—indication of NMDA receptor heterogeneity. *Neuropharmacology* 34: 533–540, 1995.

3. **Carpeggiani C, Landisman CE, Montaron MF, and Skinner JE.** Cryoblockade in limbic brain (amygdala) delays or prevents ventricular fibrillation following coronary artery occlusion in psychologically stressed pigs. *Circ Res* 70: 600–606, 1992.

4. **Cebelin MS and Hirsch CS.** Human stress cardiomyopathy: myocardial lesions in victims of homicidal assaults without internal injuries. *Hum Pathol* 11: 123–132, 1980.

5. **Ebert PA, Vanderbeck RB, Allgood RJ, and Sabiston DC Jr.** Effect of chronic cardiac denervation on arrhythmias after coronary artery ligation. *Cardiovasc Res* 4: 141–147, 1970.

6. **Elbert T, Ray WJ, Kowalik ZJ, Skinner JE, Graf KE, and Birbaumer N.** Chaos and physiology: deterministic chaos in excitable cell assemblies. *Physiol Rev* 74: 1–47, 1994.

7. **Fleiss JL.** *Statistical Methods for Rates and Proportions* (2nd ed.). New York: Wiley, 1981, p. 260–280.

8. **Friedman M, Manwaring JH, Rosenman RH, Donlon G, Ortega P, and Grupe SM.** Instantaneous and sudden deaths. *JAMA* 25: 1319–1328, 1980.

9. **Garvey JL and Melvill KI.** Cardiovascular effects of lateral hypothalamic stimulation in normal and coronary-ligated dogs. *J Card Surg* 10: 377–385, 1969.

10. **Graf BM, Vicenzi MN, Martin E, Bosnjak ZJ, and Stowe DF.** Ketamine has stereospecific effects in the isolated perfused guinea pig heart. *Anesthesiology* 82: 1426–1437, 1995.

11. **Grassberger P and Procaccia I.** Characterization of strange attractors. *Physiol Rev* 50: 346–349, 1982.

12. **Hashimi MW, Thornton JD, Downey JM, and Cohen MV.** Loss of myocardial protection from ischemic preconditioning following chronic exposure to R(−)-N6-(2-phenylisopropyl)adenosine is related to defect at the adenosine A1 receptor. *Mol Cell Biochem* 186: 19–25, 1998.

13. **Ho KK, Moody GB, Peng CK, Mietus JE, Larson MG, Levy D, and Goldberger AL.** Predicting survival in heart failure case, and control subjects by use of fully automated methods for deriving nonlinear and conventional indices of heart rate dynamics. *Circulation* 96: 842–848, 1997.

14. **Huang MH, Sylven C, Pelleg A, Smith FM, and Armour JA.** Modulation of in situ canine intrinsic cardiac neuronal activity by locally applied adenosine, ATP, or analogues. *Am J Physiol Regulatory Integrative Comp Physiol* 265: R914–R922, 1993.

15. **Huang MH, Wolf SG, and Armour JA.** Shortening of the QT interval of the EKG is associated primarily with increased ventricular contractility rather than heart rate. *Integr Physiol Behav Sci* 30: 1–11, 1995.

16. **Johansson G, Johnson L, Lannek N, Blomgren L, Lindberg P, and Pouph O.** Severe stress-cardiopathy in pigs. *Am Heart J* 87: 451–457, 1974.

17. **Kleiger RE, Miller JP, Bigger JT, and Moss AJ.** Decreased heart rate variability and its association with increased mortality after acute myocardial infarction. *Am J Cardiol* 59: 256–262, 1987.

18. **Kuller L and Lillenfield A.** Epidemiological study of sudden and unexpected death due to arteriosclerotic heart disease. *Circulation* 34: 1056–1066, 1966.

19. **Makikallio TH, Koistinen J, Jordaens L, Tulppo MP, Wood N, Golosarsky B, Peng CK, Goldberger AL, and Huikuri HV.** Heart rate dynamics before spontaneous onset of ventricular fibrillation in patients with healed myocardial infarcts. *Am J Cardiol* 83: 880–884, 1999.

20. **Makikallio TH, Ristimae T, Airaksinen KE, Peng CK, Goldberger AL, and Huikuri HV.** Heart rate dynamics in patients with stable angina pectoris and utility of fractal and complexity measures. *Am J Cardiol* 81: 27–31, 1998.

21. **Makikallio TH, Seppanen T, Airaksinen KE, Koistinen J, Tulppo MP, Peng CK, Goldberger AL, and Huikuri HV.** Dynamic analysis of heart rate may predict subsequent ventricular tachycardia after myocardial infarction. *Am J Cardiol* 80: 779–783, 1997.

22. **Malliani A, Pagani M, Lombardi F, and Cerutti S.** Cardiovascular neural regulation explored in the frequency domain. *Circulation* 84: 482–492, 1991.

23. **Meyer M, Marconi C, Ferretti G, Fiocchi R, Cerretelli P, and Skinner JE.** Heart rate variability in the human transplanted heart: nonlinear dynamics and QT vs RR-QT alterations during exercise suggest a return of neurocardiac regulation in long-term recovery. *Integr Physiol Behav Sci* 31: 289–305, 1996.

24. **Meyer M, Marconi C, Ferretti G, Fiocchi R, Mamprin F, Skinner JE, and Cerretelli P.** Dynamical analysis of heartbeat interval time series after cardiac transplantation. In: *Fractals in Biology and Medicine*, edited by Losa GA, Merlini D, Nonnenmacher TF, and Weibel E. Basel: Birkhauser, 1998, vol. 2, p. 139–151.

25. **Meyers GA, Martin GJ, Magid NM, Barnett PS, Schaad JW, Weiss JS, Lesch M, and Singer DH.** Power spectral analysis of heart rate variability in sudden cardiac death: comparison to other methods. *IEEE Trans Biomed Eng* 12: 1149–1153, 1986.

26. **Moritz AR and Zamcheck N.** Sudden and unexpected death of young soldiers. *Arch Pathol* 42: 459–494, 1946.

27. **Murphy DA, O'Blenes S, Hanna BD, and Armour JA.** Capacity of intrinsic cardiac neurons to modify autotransplanted myocardium. *J Heart Lung Transplant* 13: 847–856, 1994.

28. **Murphy DA, O'Blenes S, Hanna BD, and Armour JA.** Functional capability of nicotine-sensitive canine intrinsic cardiac neurons to modify the heart. *Am J Physiol Regulatory Integrative Comp Physiol* 266: R1127–R1135, 1994.

29. **Negoescu R, Skinner JE, and Wolf S.** Forebrain regulation of cardiac function: spectral and dimensional analysis of RR and QT intervals. *Integr Physiol Behav Sci* 28: 331–342, 1993.

30. **Oppenheimer SM and Hachinski VC.** The cardiac consequences of stroke. *Neurol Clin* 10: 167–176, 1992.

31. **Skinner JE.** Neurocardiology: brain mechanisms underlying fatal cardiac arrhythmias. *Neurol Clin* 11: 325–351, 1993.

32. **Skinner JE, Carpeggiani C, Landisman CE, and Fulton KW.** The correlation dimension of heartbeat intervals is reduced in conscious pigs by myocardial ischemia. *Circ Res* 68: 966–976, 1991.

33. **Skinner JE, Lie JT, and Entman ML.** Modification of ventricular fibrillation latency following coronary artery occlusion in the conscious pig: the effects of psychological stress and beta-adrenergic blockade. *Circulation* 51: 656–667, 1975.

34. **Skinner JE, Meyer M, Nester B, Geary U, Taggert P, Mangione A, Ramalanjaona G, Terregino C, and Dalsey W.** Comparison of linear and nonlinear analyses of heart rate variability in the prediction of mortality in patients presenting in the Emergency Department with chest pain. *Cardiovasc Res.* In press.

35. **Skinner JE and Molnar M.** Event-related dimensional reductions of the primary auditory cortex of the conscious cat are revealed by new techniques for enhancing the nonlinear dimensional algorithms. *Int J Psychophysiol* 34: 21–35, 1999.

36. **Skinner JE and Molnar M.** "Response Cooperativity:" a sign of a nonlinear neocortical mechanism for stimulus-binding during classical conditioning in the cat. *Indian Natl Sci Acad Proc.* In press.

37. **Skinner JE, Molnar M, and Tomberg C.** The point correlation dimension: performance with non-stationary surrogate data and noise. *Integr Physiol Behav Sci* 29: 217–234, 1994.

38. **Skinner JE, Pratt CM, and Vybiral T.** A reduction in the correlation dimension of heartbeat intervals precedes imminent ventricular fibrillation in human subjects. *Am Heart J* 125: 731–743, 1993.

39. **Skinner JE and Reed JC.** Blockade of a frontocortical-brainstem pathway prevents ventricular fibrillation of the ischemic heart in pigs. *Am J Physiol Heart Circ Physiol* 240: H156–H163, 1981.

40. **Skinner JE, Wolf SG, Kresh JY, Izrailtyan I, Armour JA, and Huang MH.** Application of chaos theory to a model biological system: evidence of self-organization in the intrinsic cardiac nervous system. *Integr Physiol Behav Sci* 31: 122–146, 1996.

41. **Skinner JE, Zebrowski JJ, and Kowalik ZJ.** New nonlinear algorithms for analysis of heart rate variability: low dimensional chaos predicts lethal arrhythmias. In: *Nonlinear Analysis of Physiological Data*, edited by Kantz H, Kurths J, and Mayer-Kress G. New York: Springer, 1998, p. 129–166.

42. **Stein PK, Bosner MS, Kleiger RE, and Conger BM.** Heart rate variability: a measure of cardiac autonomic tone. *Am Heart J* 127: 1376–1381, 1994.

43. **Takens F.** Detecting strange attractors in turbulence. *Lect Notes Math* 1125: 99–106, 1981.

44. **Theiler JT.** *Quantifying Chaos: Practical Estimation of the Correlation Dimension* (PhD thesis). Pasadena, California Institute of Technology, 1988.

45. **Theiler J, Eubank S, Longtin A, Galdrikian B, and Farmer JD.** Testing for nonlinearity in time series: the method of surrogate data. *Physica* D58: 77–94, 1992.

46. **Verrier RL and Dickerson LW.** Autonomic nervous system and coronary blood flow changes related to emotional activation and sleep. *Circulation* 83: II81–II89, 1991.

47. **Vybiral T and Skinner JE.** The point correlation dimension of RR-intervals predicts sudden cardiac death among high-risk patients. *Comput in Cardiol*: 257–260, 1993.

48. **Wolf SG.** Sudden cardiac death. In: *The Artery and the Process of Arteriosclerosis: Measurement and Modification*, edited by Wolf SG. New York: Plenum, 1972, p. 213–275.

49. **Wolf SG and Bruhn JG.** *The Power of Clan: the Influence of Human Relationships on Heart Disease*. New Brunswick, NJ: Transaction, 1993, p. 171.